

## 2FGL J1653.6–0159: A NEW LOW IN EVAPORATING PULSAR BINARY PERIODS

ROGER W. ROMANI<sup>1,2</sup>, ALEXEI V. FILIPPENKO<sup>3</sup>, AND S. BRADLEY CENKO<sup>4,5</sup>

*To Appear in ApJ Letters*

### ABSTRACT

We have identified an optical binary with orbital period  $P_b = 4488$  s as the probable counterpart of the *Fermi* source 2FGL J1653.6–0159. Although pulsations have not yet been detected, the source properties are consistent with an evaporating millisecond pulsar binary; this  $P_b = 75$  min is the record low for a spin-powered system. The heated side of the companion shows coherent radial-velocity variations, with amplitude  $K = 666.9 \pm 7.5$  km s<sup>−1</sup> for a large mass function of  $f(M) = 1.60 \pm 0.05$  M<sub>⊙</sub>. This heating suggests a pulsar luminosity  $\sim 3 \times 10^{34}$  erg s<sup>−1</sup>. The colors and spectra show an additional blue component dominating at binary minimum. Its origin is, at present, unclear. This system is similar to PSR J1311–3430, with a low-mass H-depleted companion, a dense shrouding wind and, likely, a large pulsar mass.

*Subject headings:* gamma rays: stars — pulsars: general

### 1. INTRODUCTION

Of 1873 0.1–100 GeV sources in the second *Fermi* Large Area Telescope (LAT) catalog, over 1170 had statistically reliable lower energy counterparts (Nolan et al. 2012). Most are blazars and spin-powered pulsars (radio-selected and Geminga-like  $\gamma$ -ray selected). Romani (2012) noted that the identification completeness of the brightest 250 LAT sources was even higher with (at that time) no more than six remaining unidentified and showed that variability and GeV spectral curvature classification flagged all six as having pulsar-like properties. Three of these sources have since been identified as millisecond pulsar (MSP) binaries with strong winds: J2339–0533, a “redback” (Romani & Shaw 2011; Kong et al. 2012), J1311–3430, a “black widow” (Romani 2012; Pletsch et al. 2013), and J1227–4859, a low-mass X-ray binary (LMXB)/MSP transition object (Ray et al. 2014). Here we report evidence that a fourth member of this set, 2FGL J1653.6–0159 (hereafter J1653), is also a MSP-driven evaporating binary.

J1653 is located at Galactic latitude  $|b| = 25^\circ$ , with a total Galactic extinction  $A_V = 0.63$  mag at this position (Schlafly & Finkbeiner 2011). With a  $22.5\sigma$  detection significance in 2FGL, an energy flux of  $F_{0.1-100 \text{ GeV}} = 3.4 \times 10^{-11}$  erg cm<sup>−2</sup> s<sup>−1</sup>, a “variability index” value of 17, and a “curvature significance” of 5.3, this is a steady source with a substantial spectral cutoff: a prime pulsar candidate. It has been searched for  $< 30$  Hz  $\gamma$ -ray pulsations (e.g., Abdo et al. 2009b) and for radio pulses to millisecond periods (Ray et al. 2014; Barr et al. 2013), with no detection. Thus, it is unlikely to be an isolated young pulsar or a persistent radio-loud MSP. We describe here an optical campaign to identify and charac-

terize a counterpart.

### 2. PHOTOMETRY AND ORBITAL-PERIOD ESTIMATE

J1653 is well localized; we used the the Goodman High Throughput Spectrograph (GHTS) at the 4.2 m SOAR telescope on 2013 August 10–12 (UT dates are used throughout) to image the 2′ radius LAT error ellipse and examine low energy counterparts. Conditions varied from poor ( $\sim 1.5''$ ) to wretched ( $> 5''$ ), and so the GHTS data were binned  $2 \times 2$ . Our strategy (as used to identify J1311 and J2339) was to obtain initial 300 s  $g'r'i'$  frames for near-simultaneous colors (Aug. 10), followed by single-color photometric sequences:  $15 \times 300$  s in  $g'$  (Aug. 10),  $29 \times 180$  s in  $r'$  (Aug. 11), and  $32 \times 300$  s in  $i'$  (Aug. 12). We were particularly interested in the eight *Chandra* X-ray sources in the revised error ellipse (see Cheung et al. 2012). Four of these had optical counterparts in our frames. The brightest X-ray source had a blue optical counterpart showing evident variability during the first hour’s observation and was thus the prime target of the light-curve study. The USNO-B1.0 position of this  $B = 20.4$  mag optical source (and likely LAT counterpart) is  $\alpha = 16^{\text{h}}53^{\text{m}}38.069^{\text{s}}$ ,  $\delta = -01^\circ58'36.71''$  (J2000.0). Although many frames had limiting magnitudes as small as  $\sim 23$ , this star was easily detected in all observations; we made sure to cover at least one maximum during each night’s photometry.

This counterpart was also observed in Gunn  $r$  (180 s) and narrow-band H $\alpha$  (600 s) with the MiniMo camera at the 3.6 m WIYN telescope on 2012 February 19. The narrow-band image did not yield a reliable magnitude, but the  $r$ -band frame could be calibrated to SDSS  $r'$ , and matched well to the SOAR light curve at the phase determined for the best-fit period (see below).

We searched image archives for exposures that may have included J1653, finding useful coverage in the Catalina Sky Survey (CSS; <http://www.lpl.arizona.edu/css/index.html>; Drake et al. 2009). These data are shallow, unfiltered, and sparse, but they show significant modulation at the orbital period. Using the SOAR, WIYN, and CSS points, we searched the folded light curves for the minimum phase dispersion with the IRAF Phase Dispersion Minimum (PDM; Stellingwerf 1978) script. This is  $P_b = 0.05194469(+10, -08)$  d, with epoch  $T_{\text{ASC}} = 56513.48078 \pm 0.00052$  (MJD). Aliases appear at

<sup>1</sup> Department of Physics, Stanford University, Stanford, CA 94305-4060, USA; rwr@astro.stanford.edu

<sup>2</sup> Visiting Astronomer, Kitt Peak National Observatory and Cerro Tololo InterAmerican Observatory, National Optical Astronomy Observatory, which is operated by the Association of Universities for Research in Astronomy (AURA) under cooperative agreement with the National Science Foundation.

<sup>3</sup> Department of Astronomy, University of California, Berkeley, CA 94720-3411, USA

<sup>4</sup> Astrophysics Science Division, NASA Goddard Space Flight Center, MC 661, Greenbelt, MD 20771, USA

<sup>5</sup> Joint Space-Science Institute, University of Maryland, College Park, MD, 20742, USA

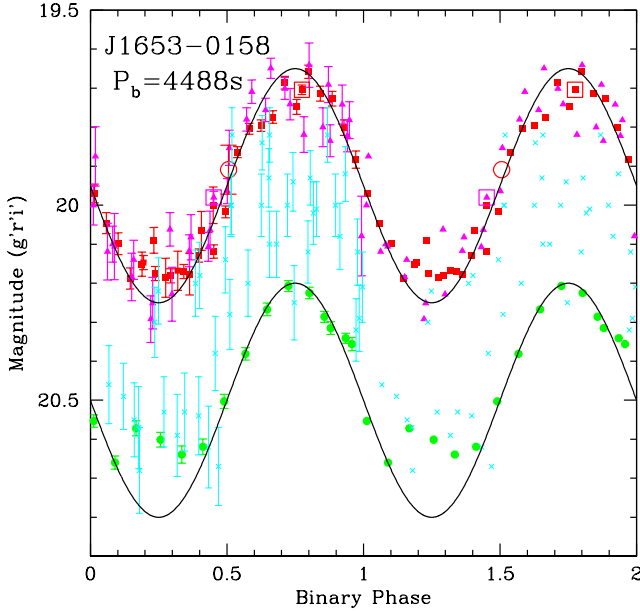


FIG. 1.—  $g'$  (circles)/ $r'$  (squares)/ $i'$  (triangles) photometry of J1653–0158, folded at the PDM-determined best-fit period. The  $r'$  and  $i'$  points from 2013 Aug. 10 are surrounded by open squares; the WIYN MiMo  $r$  point is the open circle. Two periods are shown, with error flags only during the first. CSS data (crosses) have uncertainties reduced by a factor of 2 for clarity. Simple sinusoids (with  $g' = 0.05193768d$  and  $r' = 0.05195178d$ , but these provided less satisfactory light curves. The  $P_b$  uncertainty estimate in the last two digits comes from the range of the main minimum with a PDM statistic  $\theta$  lower than that of the best sidelobe minimum. The folded light curves (two periods) are shown in Figure 1. This period,  $4488\text{ s} = 1.25\text{ h}$ , is shorter than that of any known rotation-powered pulsar binary.

For pulsar-heated companions, we expect the counterpart to be hottest (bluest) at maximum brightness. Guided by simple sinusoids, one sees that while  $g' - r'$  does decrease slightly at the peak ( $\phi_B = 0.75$ ),  $r' - i' \approx 0$  throughout the orbit. Also, the minimum is flat and the system is bluest in this region; at the light curve minimum another component dominates the light from unheated secondary. The relatively poor photometry prevents any detection of inter-orbit variability.

### 3. SPECTROSCOPY

We attempted initial spectroscopy with the GHTS and 400 line  $\text{mm}^{-1}$  grating on 2013 August 11 (MJD 56515), covering 3500–7000 Å at 7 Å resolution. With some of the best seeing of the run ( $\sim 1.3''$ ), we maintained reasonable throughput with a fixed  $1.07''$  slit. Three 600 s spectral exposures were obtained and subjected to standard calibrations, using exposures of the spectrophotometric standard EG 274. These data exhibited no strong emission lines, indicating that this was not a disk-dominated binary, and they showed a faint secondary spectrum. Cross-correlation against stellar templates revealed velocity shifts, but the low signal-to-noise ratio (S/N) and substantial velocity smearing gave large radial-velocity uncertainties.

To explore the radial-velocity variations, we obtained two exposure sequences with the Keck 10 m telescopes. First, using the DEep Imaging Multi-Object Spectrograph (DEIMOS; Faber et al. 2003) on Keck-II (2013 September 10, MJD 56545) we obtained  $12 \times 180\text{ s}$  exposure covering 4450–9060 Å with  $\sim 4.7\text{ Å}$  resolution through a  $1''$  slit. The short exposures minimized velocity smearing, and the sequence covered a full orbit. These data suggested a large radial-

velocity variation, but had low S/N and lacked blue coverage. We also observed with the Low Resolution Imaging Spectrometer (LRIS; Oke et al. 1995) on Keck-I on 2014 May 01 (MJD 56778), using the  $1''$  long-slit and the 5600 Å dichroic splitter. In the blue camera the 600/4000 grism provided coverage to  $< 3400\text{ Å}$  at  $\sim 4\text{ Å}$  resolution, while the red camera employed the 400/8500 grating at  $\sim 7\text{ Å}$  resolution. Red-side and blue-side exposures were 270 s and 330 s (respectively), and a sequence of seven exposures covered optical maximum. Observations of the spectrophotometric standards HD 84937 and Feige 34 and the radial-velocity standard HD 151288 were used in standard IRAF reductions, including optimal extraction. Again, good evidence for radial-velocity variations was apparent, but here the spectra lacked full orbital coverage.

To complete our spectroscopic study, we conducted a second campaign with Keck-I/LRIS, with the same spectroscopic configuration on 2014 May 24 (MJD 56802). For both LRIS campaigns we set the slit at PA =  $+20^\circ$  to include a star of comparable brightness  $29''$  south-southwest. Monitoring this G-type field star and the night-sky lines allowed us to confirm the stability of the radial-velocity solution and to connect photometry and velocity measurements between the observing runs. In this run we obtained a sequence of  $43 \times 240\text{ s}$  exposures with the red camera, binned a factor of 2 in the spatial direction to minimize the readout time. The blue camera was run unbinned, and exposure times were adjusted (250–285 s, typically 265 s) to keep the exposure midpoints approximately aligned with those of the red camera. These observations covered three orbits; we also obtained exposures of spectrophotometric standards and the G/K radial-velocity standards HD 122120, HD 125184, and HD 125455.

A failure of the blue camera shutter early in the sequence allowed counts to accrue during readout, adding up to  $\sim 7\%$  continuum contamination at 5500 Å, less to the blue. Using a blue standard observed before shutter failure and cross-calibrating with the field star (referenced to the 2014 May 01 average spectrum), we developed a stable spectrophotometric solution. The red camera was not affected. Residual mismatch across the dichroic wavelength suggests that the absolute spectrophotometry for  $\lambda < 5550\text{ Å}$  has an additional  $\sim 20\%$  uncertainty beyond the usual variable slit losses.

#### 3.1. Orbital Variations

Our study of the orbital variations starts with a comparison of spectra at maximum brightness (“Day”;  $0.6 < \phi_B < 0.9$ ; 14 exposures) and minimum brightness (“Night”;  $0.1 < \phi_B < 0.4$ ; 13 exposures). Figure 2 shows average spectra from these windows, Doppler shifted to the rest frame according to the best radial-velocity solution (see below). Although the true extinction is not well known, we have dereddened using the full Galactic  $A_V = 0.63\text{ mag}$ , consistent with the X-ray spectrum (§4). “Night” is dominated by a nearly power-law component ( $F_\lambda \propto \lambda^{-1.1 \pm 0.1}$ ); the step at  $\sim 5500\text{ Å}$  likely represents residual flux-calibration uncertainties. With a lower  $A_V = 0.3\text{ mag}$ , the spectrum fits somewhat less well as a power law with index  $-0.75 \pm 0.2$ . The maximum-light “Day” spectrum includes a thermal excess (Diff), plotted along with main-sequence K5 ( $T_{\text{eff}} \approx 4400\text{ K}$ ) and F2 ( $T_{\text{eff}} \approx 6900\text{ K}$ ) comparison spectra. The thermal excess is broader than a stellar spectrum, evidently from the range of  $T_{\text{eff}}$  over the heated “Day” face of the companion star. Low-S/N difference spectra at quadrature (“Dawn” and “Dusk”)

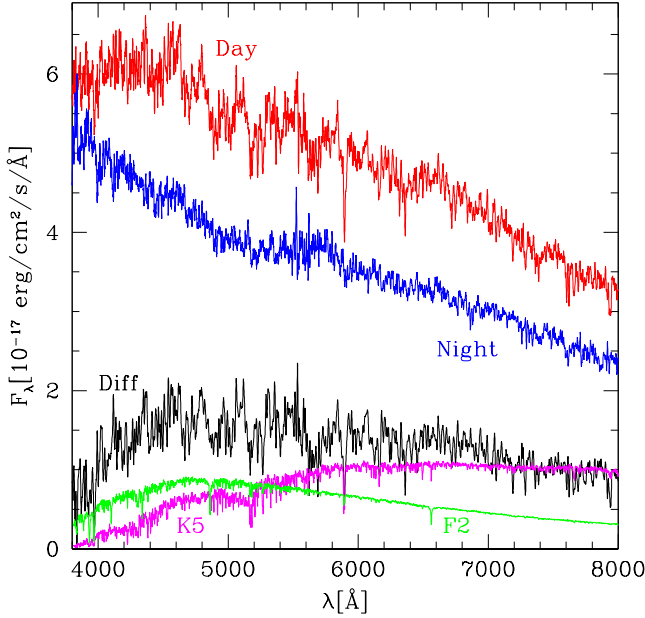


FIG. 2.— Keck-I/LRIS spectra of J1653–0158, showing maximum-brightness (“Day”;  $0.6 < \phi_B < 0.9$ ) and minimum-brightness (“Night”;  $0.1 < \phi_B < 0.4$ ) average spectra after dereddening and shifting to the best-fit radial-velocity curve. The “Day”-side thermal excess is compared with two main-sequence stellar spectra.

give lower effective temperatures. The “Dusk” thermal excess appears brighter and hotter than that during “Dawn,” but this is presently of low significance; such asymmetry can be explored using simultaneous multi-color photometry. The “Night” spectrum shows no spectral features; we find equivalent-width limits  $< 0.3 \text{ \AA}$  for kinematic line width below  $\sim 10 \text{ \AA}$ . The nature of this blue emission is unclear. In contrast, the “Day” spectrum exhibits many broad and narrow absorptions matching standard stellar spectral features. A number of the strongest metal lines can be individually identified in the “Day” average. Hydrogen Balmer lines are not detected. Comparing with SDSS normal-star spectra, we find equivalent-width limits of  $H\alpha$ ,  $H\beta$ , and  $H\gamma$  to respectively be  $< 0.07, 0.11, 0.14 \text{ \AA}$  in the “Day” spectrum versus  $1.04, 0.66, 1.16 \text{ \AA}$  (K5 V) and  $3.17, 4.15, 2.69 \text{ \AA}$  (F2 V). The equivalent widths should, however, be measured for the thermal component of the spectrum; the limits for the lower-S/N difference spectrum are  $< 0.4 \text{ \AA}$  for all three species. Thus, H is weaker than in normal stars by a factor of 2–10 in this Diff spectrum, depending on which  $T_{\text{eff}}$  dominates the “Day”-side excess. While less impressive than for PSR J1311–3430, whose strongly heated face shows a limit  $[H] < 10^{-5}$  of normal, it appears that this companion may have also lost appreciable hydrogen. We do not detect individual He I lines, but this is not surprising for the  $T_{\text{eff}}$  range seen here. Na I  $\lambda 5892$  is, as for PSR J1311–3430, very strong compared to the comparison stars.

### 3.2. Orbital Radial Velocities

We can use the line features on the heated face to estimate the companion radial velocity. The measurements were made via cross-correlation, using the IRAF XCASO script (Kurtz & Mink 1998). We used the wavelength range 3500–10,000  $\text{\AA}$  after excising regions near strong night-sky lines and the immediate vicinity of the dichroic transition. The bulk of the correlation significance stems from the metal line features at 4000–5500  $\text{\AA}$ , but significant and consistent correlation signal was also measurable in the red portions of the

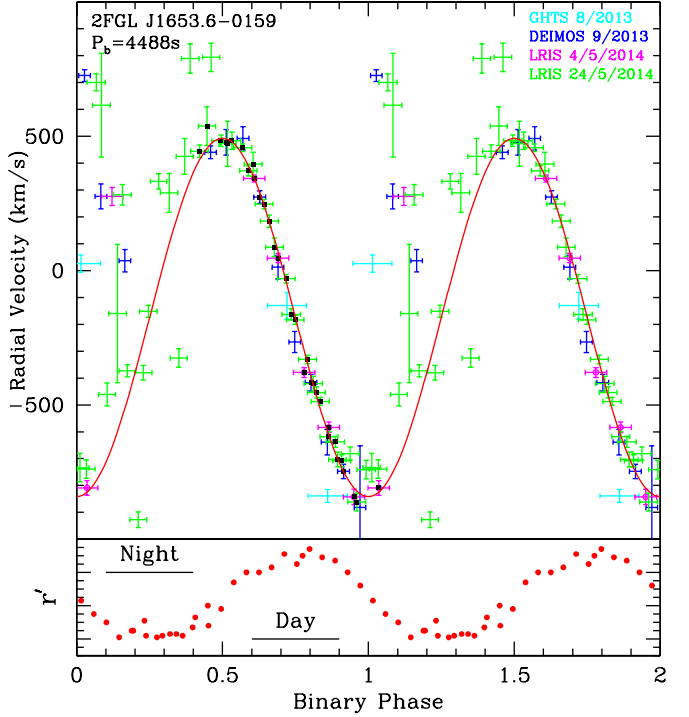


FIG. 3.— Radial velocities measured by cross-correlation of a K5 V template plotted on the photometric ephemeris of §2. The  $r'$  light curve is plotted at bottom for reference and two periods are shown. Points with black dots are used to fit  $K_2$  and  $\Gamma$  for the simple sinusoid, shown by the line.

spectra. A range of stellar templates was used. While significant correlations and similar  $v_r$  were obtained using early-M through F templates, the best correlations were obtained with K-type spectra. We report here the results for a K5 V template. Monitoring the night-sky lines during each campaign and comparing the radial-velocity fits to the comparison field star between Keck campaigns showed that our wavelength solutions are stable to  $0.1 \text{ \AA} \approx 5 \text{ km s}^{-1}$ . Correlations against the radial-velocity standards imply a similar accuracy for the absolute  $v_r$ .

The cross-correlation significance is monitored via the  $R$  statistic. For the May 24 data, the individual spectra near optical maximum had  $R \approx 7$ –10 with radial-velocity accuracies  $\sigma_{v_r} \approx 15$ –20  $\text{km s}^{-1}$ . Near quadrature the accuracies dropped to  $\sim 30 \text{ km s}^{-1}$ . Since “Night”-side spectra lack stellar features, the cross-correlation showed low significance with  $R < 2$ . Although we do find similar “Night” velocities at a given phase from the various observing runs, there is little systematic velocity trend and essentially all the correlations are of low significance. This suggests that the “Night” phase velocities, even when they show modest statistical errors, are generally not meaningful.

The cross-correlation velocities from our four spectroscopic campaigns are shown in Figure 3, phased to the photometric ephemeris. Over the phase range  $0.4 < \phi_B < 1.1$ , the velocity errors are small and, with a few outliers, the measurements from the various instruments are in good agreement. We performed a weighted least-squares fit to the measurements with  $R > 3$  in this phase range. Two 2014 May 24 LRIS points, at  $\phi_B = 0.94$  with  $R = 6.1$  and  $\phi_B = 0.99$  with  $R = 4.0$ , lay several sigma from all best-fit curves. Excluding these points, the fit uses the measurements marked with a black central dot in Figure 3 and results in a secondary velocity amplitude  $K_2 = 666.9 \pm 7.5 \text{ km s}^{-1}$  and mean velocity  $\Gamma = -174.6 \pm 5.1 \text{ km s}^{-1}$  with a fairly good  $\chi^2/\text{DoF} = 1.75$ .

Inclusion of the two dropped points decreases  $K_2$  by  $1.3\sigma$  and  $\chi^2/\text{DoF}$  grows to 2.52. Note that several low significance points in the range  $0.9 < \phi_B < 1.1$  also lie  $\sim 70 \text{ km s}^{-1}$  redward of the best-fit curves. This, plus the light-curve asymmetry and bluer spectrum at this phase, suggest some heating/wind activity in the “Dusk” region, which may perturb the photospheric radial velocities. Similar, but dramatically stronger effects are seen for J1311–3430 (Romani et al. 2014).

Our measured  $0.4 < \phi_B < 1.1$  radial velocities follow the center of light of the secondary star, weighted by a K5 V spectrum. The resulting mass function,

$$f(M) = \frac{PK_2^3}{2\pi G} = \frac{M_1^3 \sin^3 i}{(M_1 + M_2)^2} = 1.60 \pm 0.05 M_\odot,$$

is a strict lower limit for the mass of the presumed pulsar. This value (the largest for any evaporating black-widow or redback-type pulsar) makes it virtually certain that the unobserved, heat-producing object is a neutron star. It is unlikely that the blue spectrum seen at optical minimum is photospheric emission from a white-dwarf primary, in accord with the lack of spectral features and the sub-Rayleigh-Jeans spectral index. Since the center of light of the heated face is inside the secondary center of mass and since  $\sin i < 1$ , the true primary mass is likely substantially higher.

#### 4. ARCHIVAL X-RAY DATA

Our counterpart, source 38 in the 21 ks *Chandra X-ray Observatory* ACIS observation of Cheung et al. (2012), provides  $\sim 350$  X-ray photons. We fit these data to a power-law model with *CIAO/SHERPA*, finding a photon index  $\Gamma = 1.65_{-0.34}^{+0.39}$ , absorption  $N_H = 1.3_{-1.3}^{+1.8} \times 10^{21} \text{ cm}^{-2}$ , and unabsorbed flux  $1.9_{-0.6}^{+0.9} \times 10^{-13} \text{ erg cm}^{-2} \text{ s}^{-1}$  (0.5–8 keV,  $\chi^2_G$  statistic, 90% uncertainty), in agreement with the Cheung et al. (2012) measurements. Note that  $A_V = 0.63 \text{ mag}$  corresponds to  $N_H \approx 1.2 \times 10^{21} \text{ cm}^{-2}$ , so the X-rays suggest that J1653 is seen through much of the Galactic dust layer. Improved measurements are needed to pin down the extinction and distance. We folded the X-ray counts on the photometric ephemeris and find no evidence for an eclipse or for any orbital variation, although given the limited counts, shallow modulation could have been missed. A similar fold of the LAT GeV photons also shows no evidence for orbital modulation.

#### 5. SYSTEM MODELING AND CONCLUSIONS

Lacking kinematic constraints from  $\gamma$ -ray or radio timing, our picture of J1653 is still imprecise. Some basic pulsar scaling laws can, however, be used to check consistency with the evaporating binary scenario. First,  $\gamma$ -ray pulsars have a heuristic luminosity  $L_{\gamma, \text{heu}} \approx (\dot{E} \times 10^{33} \text{ erg s}^{-1})^{1/2}$  (Abdo et al. 2010). Next, X-ray emission from rotation-powered pulsars scales as  $L_X \approx 10^{-3} \dot{E}$  (Becker 2009). The observed fluxes  $f_\gamma$  and  $f_{X, \text{unabs}}$  then give estimates of  $\dot{E} \approx 3 \times 10^{34} \text{ erg s}^{-1}$  and  $d \approx 1.1 \text{ kpc}$ . Breton et al. (2013) describe how pulsar spin-down flux (assumed isotropic at separation  $a$ ) heats the companion from a “Night”-side  $T_N$  to a maximum  $T_D$  according to

$$\eta \dot{E} \approx 4\pi a^2 \sigma (T_D^4 - T_N^4),$$

finding a typical efficiency  $\eta \approx 0.15$  for black-widow systems. For J1653, we have  $a \approx K_2 P_B / 2\pi \approx 0.7 R_\odot$  and  $T_D \gg T_N$ , so we can expect  $T_D \approx 5500 \text{ K} (\eta_{0.15} \dot{E}_{34})^{1/4}$ .

The effective  $T_D$  is not well measured, but from our spectroscopy it seems lower than 6500 K. This implies  $\eta_{0.15} \dot{E}_{34} \approx 2$ , somewhat lower than the  $f_\gamma/f_X$  estimate above, and suggesting a smaller  $d \approx 0.8 \text{ kpc}$  as well. Finally, the extinction-corrected optical flux from the heated face (Diff spectrum) is  $f_{\text{opt}} \approx f_{-13} 10^{-13} \text{ erg cm}^{-2} \text{ s}^{-1}$  with  $f_{-13} \approx 0.9$  using the bolometric correction for 6000 K. From this we derive an effective companion radius of  $R_* \approx (4f_{\text{opt}}/\sigma)^{1/2} d/T_{\text{eff}}^2 \approx 0.10 f_{-13}^{1/2} d_{\text{kpc}} / (T/6000 \text{ K})^2 R_\odot$ . This gives  $R_*/a \approx 0.13 d_{\text{kpc}} / T_{6000}^2$ , which can be compared with the Roche radius  $R_{L2}/a \approx 0.46 q^{-1/3}$ . For a redback-type mass ratio  $q \approx 10$  this gives  $R_{L2}/a \approx 0.2$ , so the companion would be well inside the Roche lobe. For a black-widow-type mass ratio  $q \approx 100$ ,  $R_{L2}/a \approx 0.1$ , so the companion fills the Roche lobe, even for somewhat larger  $T_{\text{eff}}$ , smaller  $A_V$ , and smaller  $d_{\text{kpc}}$ .

We would like to improve the mass and fill-factor estimates. The absence of X-ray or  $\gamma$ -ray eclipses implies  $i < 85^\circ$ , so the minimum pulsar mass ( $K_2$  lower limit) is  $1.62 M_\odot$  for a substellar (black-widow-type) companion. For a redback-type  $\sim 0.2 M_\odot$  companion, the limit is  $M_{\text{PSR}} > 1.92 M_\odot$ . One generally refines the constraints on the center-of-light to center-of-mass correction factor  $K_{\text{cor}} = K_{\text{CoM}}/K_{\text{CoL}}$  and the inclination  $i$  via light-curve modeling. This is important since  $K_{\text{cor}} > 1$  and the pulsar mass grows as  $M_{\text{PSR}} \propto (K_{\text{cor}}/\sin i)^3$ . At present such modeling is not very constraining since our photometry is poor and nonsimultaneous. Additional observations can, of course, remedy this.

More important, though, are the apparently nonthermal flux which dominates the optical light at minimum brightness and the possible light-curve asymmetries near maximum brightness. These suggest that a strong evaporating wind distorts the light curve and makes it difficult to detect the companion at minimum brightness. Simple heating models may not be adequate. This also appears true for other black-widow systems with well-studied light curves, J1311 (Romani et al. 2014) and PSR J1544+4937 (Tang et al. 2014). Improved understanding of evaporative winds and their effect on the light curves seem crucial for refined measurements of the short-period black widows. J1653 certainly motivates such efforts: the small  $P_b$ , peculiar companion composition, and likely large  $M_{\text{PSR}}$  all flag this as an extreme member of the evaporating-pulsar population. Once  $\gamma$  and/or radio pulses are detected, we plan to pursue such studies.

We thank Sasha Brownsberger and Matt Stadnik for assistance with the photometric observations, and Melissa Graham, Patrick L. Kelly, and WeiKang Zheng for assistance with the spectroscopic observations. This work was supported in part by NASA grant NNX11AO44G. A.V.F. was supported by the Richard & Rhoda Goldman Fund, the Christopher R. Redlich Fund, the TABASGO Foundation, and NSF grant AST-1211916. This research is based in part on observations obtained at the Southern Astrophysical Research (SOAR) telescope, which is a joint project of the Ministério da Ciência, Tecnologia, e Inovação (MCTI) da República Federativa do Brasil, the U.S. National Optical Astronomy Observatory (NOAO), the University of North Carolina at Chapel Hill (UNC), and Michigan State University (MSU). Some of the data presented herein were obtained at the W. M. Keck Observatory, which is operated as a scientific partnership among the California Institute of Technology, the University of California, and NASA; the Observatory was made possible by the

generous financial support of the W. M. Keck Foundation.

#### REFERENCES

- Abdo, A. A., et al. 2009b, *Science*, 325, 840  
 Abdo, A. A., et al. 2010, *ApJS*, 187, 460.  
 Barr, E. D., et al. 2013, *MNRAS*, 429, 1633  
 Becker, W. 2009, *ASSL*, 357, 91  
 Breton, R. P., et al. 2013, *ApJ*, 769, 108  
 Cheung, C. C., et al. 2012, *ApJ*, 756, 33  
 Drake, A. J., et al. 2009, *ApJ*, 696, 870  
 Faber, S. M., et al. 2003, *SPIE*, 4841, 1657.  
 Kong, A. et al. 2012, *ApJ*, 747, L3.  
 Kurtz, M. J., & Mink, D. J. 1998, *PASP*, 110, 934  
 Oke, J. B., et al. 1995, *PASP*, 107, 375  
 Nolan, P. L., et al. 2012, *ApJS*, 199, 31  
 Pletsch, H. J., et al. 2012, *Science*, 338, 1314  
 Ray, P. S., et al. 2012, *arXiv1205.3089*  
 Ray, P. S., et al. 2012, 2014HEAD...1412226  
 Romani, R. W. 2012, *ApJ*, 754, L25  
 Romani, R. W., & Shaw, M. S. 2011, *ApJ*, 743, L26  
 Romani, R. W., et al. 2012, *ApJ*, 760, L36  
 Romani, R. W., et al. 2014, *ApJ*, in prep.  
 Schlafly, E. F., & Finkbeiner, D. P. 2011, *ApJ*, 737, 103  
 Stellingwerf, R. F. 1978, *ApJ*, 224, 953  
 Tang, S., et al. 2014, *ApJ*, submitted; *ArXiv* 1407.0081v2